Available online at www.sciencedirect.com

SciVerse ScienceDirect

Ceramics International 39 (2013) 2683–2693

CERAMICS INTERNATIONAL

www.elsevier.com/locate/ceramint

Influences of evaluation methods and testing load on microhardness and Young's modulus of ZTA and ATZ ceramics

Vincenzo Tebaldo*, Giovanna Gautier

National Research Council, Institute for Agricultural and Earthmoving Machines, Strada delle Cacce 73, 10135 Turin, Italy

Received 15 June 2012; received in revised form 4 September 2012; accepted 10 September 2012
Available online 26 September 2012

Abstract

In this work, microindentation tests under different conditions were performed to determine the influence of indentation load on Young's modulus and microhardness of ZrO_2 reinforced with Al_2O_3 particles (ATZ) and Al_2O_3 reinforced with ZrO_2 particles (ZTA).

Microhardness of ATZ and ZTA materials was measured using traditional Vickers and instrumented microhardness methods at 500, 1000, 1500 and 2000 mN loads. As for the instrumented method, Vickers microhardness was calculated from the force-indentation depth curves by analyzing the unloading segments, according to the Oliver–Pharr method. In this way the possible differences between the two methods were calculated. Furthermore, Young's modulus at each load was calculated using the instrumental method.

The main differences between the two methods were analyzed, and the influence of the load on the definition of Young's modulus in the case of the instrumental method was studied. The results indicated an indentation load effect for both materials, as hardness and Young's modulus increase by decreasing the indentation load.

Keywords: Ceramic composites; Microhardness; Young's modulus; Martens hardness

1. Introduction

In previous years there was an increasing use for oxidic materials within biomedical fields, especially in dentistry and prosthetic, e.g. for load bearing and wear resistance applications. However the results have not always met the expectations because of their fragility, causing sometimes the prosthesis failure. For example, Linkevicius et al. [1] have shown how particular ceramic materials exhibit a tendency to fracture when subjected to high compression conditions. For this reason, the need for ceramics showing a good balance between hardness and toughness has increased.

This balance can be achieved by using zirconia-based ceramic, as the tetragonal form of zirconia has excellent mechanical properties. However since the thermodynamically stable form of pure zirconia is monoclinic at room temperature, tetragonal zirconia is subjected to phase transformation during cooling, causing an increase in volume sufficient to cause a failure [2,3].

For this reason, pure zirconia is stabilized by oxides such as Y_2O_3, which allows the maintenance of the tetragonal structure at room temperature. In spite of the stabilization, zirconia is subjected to aging in the presence of water [4] which leads to the degradation of the surface.

A good compromise is to use the alumina–zirconia composites as an alternative to pure zirconia. Two types of ceramic composites can be prepared: the first consisting of a matrix of ZrO_2 reinforced with alumina particles, called ATZ (developed for its excellent value hardness–toughness), and the second consisting of a matrix of Al_2O_3 reinforced with particles of zirconium oxide, known as ZTA (developed to substitute alumina ceramics in applications where a higher fracture resistance was required).

De Aza et al. [5] have shown that in both cases, the fracture toughness of the ceramic material has increased with respect to the monolithic form. Based on the importance of such composites, the study of their properties is very important for a proper application. For this reason,

*Corresponding author. Tel.: +39 011 3977622.
E-mail address: v.tebaldo@ima.to.cnr.it (V. Tebaldo).

0272-8842/$ - see front matter © 2012 Elsevier Ltd and Techna Group S.r.l. All rights reserved.
http://dx.doi.org/10.1016/j.ceramint.2012.09.035

an analysis of the methods to measure hardness and Young's modulus is needed.

The definition of hardness, as already known, is the resistance of a material to permanent penetration by another harder material. As for microhardness, the procedure involves the application of a fixed load on a diamond indenter and the measurement, with the help of a microscope, of the size of the indentation on the material surface after unloading, so that the elastic deformation of the material is ignored.

In the past, the microhardness of a material was evaluated by different methods, the most common of which is the traditional Vickers. By this test the measured microhardness depends on the test load and dwell times. However, this method involves some uncertainties due to the inaccuracy of the optical measurements and the perception of the operator [6].

A further contribution to the uncertainty in the measurement of microhardness on ceramics are cracking and chipping of the samples. The characteristics of ceramic materials, such as surface roughness due to the porosity in the volume and to the presence of multiple phases with different hardness, affect the shape of the indentation so that the normal procedure of analysis can lead to some uncertainty in the hardness values [7].

For these reasons, in recent years a more modern approach has gained considerable interest, especially when the optical evaluation is extremely difficult as in the case of hard materials. This method, formerly known as the universal microhardness test, is now called the Martens test and it is suitable for testing the microhardness of most hard materials [8]. In this case the microhardness value comes from the indentation depth under working load and it is therefore less affected by the material's visco-elastic and optical properties [9].

The Martens test, also called instrumented test, unlike traditional tests, provides the ability to continuously measure the indenter penetration under the applied load during the test cycle. Martens hardness data is the one indentation parameter which gives one number that characterizes the material's complex resistance to the total elastic–plastic deformation. In this way it is possible to measure the elastic and plastic deformation of materials using the initial slope of the unloading curve. For this reason, the so determined hardness is not equivalent to the hardness previously defined as the resistance to the permanent deformation.

Depth-sensing indentation method has become a very useful technique for measuring Young's moduli and hardness of sintered ceramics and materials of small volume [10].

Krell et al. [11] noted that the microhardness varies with the indentation load in the case of alumina, where microhardness generally presents an indentation size effect. This effect is considered to be dependent on a variety of phenomena, including work hardening during indentation and the load at which plastic deformation begins [10].

Based on the growing interest in the use of ceramic materials, the aim of this paper is to provide an assessment of the influence, if any, of the indentation load on microhardness and Young's modulus of sintered ATZ and ZTA ceramics using a microindentation technique at small indentation loads (500–2000 mN).

In order to compare the values, the microhardness of the samples was obtained by two methods, i.e. the traditional Vickers and the instrumented one. In the last case, Vickers hardness was calculated by the force-indentation depth curves, recorded during Martens hardness measurements, using the Oliver and Pharr method [12].

In both the cases, the geometry of the indenter is the same but the testing process is different and when you have to evaluate the surface properties of a material, one may be more appropriate than the other.

According to the standards that govern the universal and traditional microhardness test, the results must be expressed in GPa, with regard to the instrumented hardness, and in N/mm^2, for optically determined hardness values [11]. However, for an easier comparison of the results, in this paper both will be expressed in GPa.

2. Experimental procedure

2.1. Samples preparation for the analysis

Two kinds of ceramic composites were considered:

- An yttria stabilized zirconia matrix reinforced with alumina particles, alumina toughened zirconia (ATZ);
- an alumina matrix reinforced with zirconia particles, zirconia toughened alumina (ZTA).

The overall production process of these ceramic materials consists of the following steps:

- forming of a green specimen;
- sintering of the green sample.

The following raw powders ''ready to press'' were used:

- for ZTA the granulated powder was an alumina composite (pure at 99.99%), with 84% in weight of alumina and 16% of zirconia, (Taimei Chemicals: Al_2O_3–16%ZrO_2 Taimicron)
- for ATZ the powder was a composite of zirconia with 20% in weight of alumina (Tosoh Corporation: ZrO_2–20%Al_2O_3, TZ-3Y20AB).

In both cases, the zirconia powders contain 3 mol% of yttria (~4 wt%), required to stabilize the tetragonal zirconia during the sintering, and traces of other compounds.

Green samples were produced using the following pressing procedure:

1. Uniaxial Pressing at low pressure, around 49 MPa; at this step the powders were pressed in a stiff die, by

means of a piston which applies the pressure only in one axial direction;
2. afterwards, the samples were subjected to Cold Isostatic Pressing (CIP) at a pressure of 245 MPa for 1–2 min; in the CIP the pressure is applied through a fluid on a gum mould filled up with the powder and is therefore uniformly distributed in all the directions of the green body to obtain uniform density distribution

The forming phase was carried out in moulds of proper dimensions to obtain final green compacts of 33×33 mm^2, thickness 11 mm with parallel surfaces as for ISO guidelines for Martens microhardness test [13]. The green compacts have been then sintered. For the sintering process, the following cycle was used: heating up to 700 °C with a ramp rate of 50 °C/h, permanence at 700 °C for 2 h; then a heating up at a rate of 100 °C/h up to the final sintering temperature (1500 °C), permanence at 1500 °C for 2 h. Table 1 shows the values of resulting absolute density, relative density and average grain size of Al_2O_3 and ZrO_2 phases. For the evaluation of average grain sizes, the samples were thermal etched and analyzed by SEM. The linear intercept method was used and 100 measurements were made by using SEM images, by means of which it has managed to calculate a sufficiently accurate average. Average grain sizes were determined using the following equation:

$G=(-6.6457 \log_{10} Lm)-3.298$ where Lm is the mean linear intercept [14].

Sintered specimens were then mirror polished using different diamond suspensions and proper disks. Different disks were used (using diamond pastes of 9, 3, and 1 μm particle size) in order to progressively reduce the roughness up to 0.025 μm, so that the sample surface was polished at a roughness suitable for the analyses. At this step the sample was ready for microhardness tests.

2.2. Roughness

In order to improve the accuracy of microhardness test measurements, according to ISO 14577, the roughness of the sample has to be below the limit of 5% of the maximum penetration depth.

The average roughness (*Ra*) value was calculated using a Form Talysurf 120 profilometer (IMAMOTER-CNR, Turin, Italy) under the following conditions:

Cut off length = 0.8 mm
Cut off number = 3
Length of measurement = 2.4 mm

The stylus type was conical, with a radius tip of 2 μm. The tests were performed within an air-conditioned laboratory, where the temperature is kept at 20 °C. Twenty measurements were made for each sample, randomly, within an area whose sides were at a distance of 4 mm from the edges of the specimen.

The surface preparation was considered appropriate when the arithmetic mean roughness *Ra* was less than 0.08 μm. To perform the high quality of reference blocks the arithmetic mean roughness *Ra* was minimized down to 0.02 μm.

2.3. Martens and Vickers microhardness by depth-sensing measurements

Martens microhardness was determined by a FISCHERSCOPE HM 2000 XYm (Fischer, NIS-University of Turin, Turin, Italy) with the WIN-HCU software. It is a computer-controlled measuring system for microhardness testing and determination of material parameters according to the standard ISO 14577 [13]. The main technical parameters of this instrument are:

Operation control mode: Force
Test load range: 0.4–2000 mN
Load resolution: 4×10^{-2} mN
Distance resolution: 0.1 nm

Martens microhardness test consists to force the vertex of a diamond indenter into the surface of a sample and to measure the indentation depth under a testing force maintained for 20 s.

The indenter used has a pyramid shape, with a square base (vertex angle equal to 136°). The test may be conducted by controlling the test force or by controlling the indentation depth h. In both cases the force and depth are measured and recorded continuously, both during increasing load as well as during decreasing test load.

The indenter displacement represents the sum of the elastic displacement of the sample surface at the perimeter of the contact and the plastic depth of the impression [9]. A distance at least 100 times greater than the indentation depth was kept between the edge of the sample and the center of each indentation.

After the head touches the specimen, the approach speed of the indenter until zero-point is ≤ 2 μm/s. For the Fischerscope HM 2000 XYm, the zero point was automatically detected during the indentation process by the software belonging to the instrument.

Table 1
Density and grain size of ATZ and ZTA.

	Absolute density (g/cm^3)	Relative density (%)	Average grain size (μm)
ATZ	5.478	99.9	$Al_2O_3-ZrO_2 \rightarrow 0.469 \pm 0.174$
ZTA	4.183	100	$Al_2O_3 \rightarrow 0.881 \pm 0.297$ $ZrO_2 \rightarrow 0.317 \pm 0.103$

Before any test, calibration was performed onto an acrylic plate to ensure that the results were within the normal range of reproducibility.

The tests were carried out at loads of 500, 1000, 1500 and 2000 mN. Ten indentations for each load were made to account for the scatter caused by residual porosity or foreign particles. Each test was performed to give a cycle with the same rates on loading and unloading, using the following conditions:

- Peak load of 500 mN, loading rate of 25 mN s^{-1}
- Peak load of 1000 mN, loading rate of 50 mN s^{-1}
- Peak load of 1500 mN, loading rate of 75 mN s^{-1}
- Peak load of 2000 mN, loading rate of 100 mN s^{-1}

These loading rates allow reaching the final peak within 20 s. A dwell time of 5 s at maximum load was used to check for residual creep.

The Martens microhardness was measured automatically by the software as test force F divided by the surface area of the indenter $A(h)$ penetrating beyond the zero-point (point of the first contact of the indenter with the test-piece surface) and expressed as N/mm^2:

$$HM = \frac{F}{A(h)}$$

Oliver et al. [12] showed that the $A(h)$ is determined from the so-called area function of the indenter tip, $A(h)=f(h_c)$ where h_c is the contact depth, i.e. the distance, measured along the indenter axis, of the indenter in contact with the sample. The indentation depth h_c is related to the maximum indentation depth, h_{max}, by the equation: $h_c = h_{max} - \varepsilon\left(F_{max}/S\right)$, where ε is a constant depending on the geometry of the indenter and S is the contact stiffness, defined as an increment in load divided by the resulting increment in displacement in the absence of plastic deformation.

The unloading curve fit is analytically differentiated to determine the slope at maximum load:

$$S = \frac{dF}{dh} \quad \text{at } F = F_{max}$$

After determining the depth of contact you can obtain the contact area by the geometry of the pyramid:

$$A(h) = \frac{4\sin\alpha/2}{\cos^2\alpha/2} h_c^2$$

where α is the angle between opposite faces of vertex of the pyramid.

For a perfect Vickers indenter the contact area $A(h)$ can be calculated as follows:

$$A(h) = 26.43 h_c^2$$

The test result is a force/indentation depth curve. Since this curve includes both the elastic and plastic response of the tested material, it can be used to derive a number of parameters that describe the behavior of the material.

The force–depth indentation (P–h) curves generated by the Martens tests were used to determine Vickers hardness values using the method introduced by Oliver and Pharr [12]. The plastic deformation can be calculated from the separation of the elastic deformation from the total recorded deformation by using the initial unloading slope S:

$$HV_{L-D} = \frac{F_{max}}{26.43(h_{max} - \varepsilon F_{max}/S)^2}$$

where $\varepsilon = 0.75$, $F = m(h - h_0)^n$ and $S = nm(h_{max} - h_0)^{n-1}$. The coefficients m and n are the fitting coefficients for the unloading curve, n is the power of the curve and m is the power law prefactor. The HV_{L-D} values obtained by this method were compared with traditional Vickers values and any differences were statistically evaluated.

2.4. Traditional Vickers microhardness

Microhardness measured by traditional Vickers method depends on the test load and dwell times. By this method the microhardness is evaluated only after the removal of the applied load by optical measurements of the diagonals of the residual indent.

Although diamond indenter shows a very high elasticity modulus and hardness, its elastic deformation during penetration can be substantial, based on the mechanical properties of the material. Bouzakis et al. [15] have shown the influence of the deviations induced by the indenter deformation according to the mechanical properties of the sample.

Vickers microhardness is expressed as a function of the applied load F and the diagonal of the indent d according to the following expressions:

$$HV = 1854.4 \frac{F}{d^2}$$

where HV is the Vickers Hardness (in GPa) with F in Newton and d in micrometer. The constant value 1854.4 arises from the calculation of the contact area.

The traditional Vickers hardness tests were carried out using a Durimet microhardness tester (IMAMOTER-CNR, Turin, Italy) under 500, 1000, 1500, 2000 mN loads and the indent diagonals were measured using a scanning electron microscope (SEM, 2i3T University of Turin, Turin, Italy). Ten indentations were made for each load with dwell time of 20 s: eight at a distance of 5 mm between the center of each indentation and the edge of the specimen and two in the center of the specimen at a distance of 11 mm from the center of the other indentations.

2.5. Young's modulus

The slope S originated from the elastic recovery of the deformed material can be estimated from the unloading curve at the peak load F_{max}. The measured slope increases by rising Young's modulus of the material and can be used

for calculating the indentation modulus as an approximation to the Young's modulus. Krell et al. [16] showed that the measurement of the slope of the tangent to the upper part of the unloading curve is often difficult to be determined, inducing some errors in the evaluation of Young's modulus. For this reason, Young's modulus of the specimens can be extracted according to the following relation:

$$\frac{1}{E_r} = \frac{1-\upsilon^2}{E} + \frac{1-\upsilon_i^2}{E_i}$$

where E_i and υ_i are Young's modulus and Poisson's ratio of the diamond indenter and E and υ are the same quantities for the specimens. The indenter properties used for all calculations were E_i=1141 GPa and υ_i=0.07. This approach allows to avoid the problems arising from the difficulty in measuring the precise slope of the tangent of the unloading curve.

E_r is the reduced modulus, derived from the equation:

$$\frac{dF}{dh} = \beta \frac{2}{\sqrt{\pi}} \sqrt{A} \times E_r$$

where A is indenter area, dF is the load increment and dh is the increment of the indentation depth in the range of 60–95% of maximum load for unloading curve. β is a numerical factor whose value is 1.012 for a square indenter [10].

3. Results and discussion

After the process of mirror polishing of the ceramic samples, both materials show similar surface average roughness, in the range of 0.0172–0.0177 μm with standard deviation of 0.0019 for ATZ and 0.0030 for ZTA.

As described previously, the penetration of the indenter can be influenced by cracking or chipping during testing, which occur more often at higher applied loads.

The presence of cracking can affect the shape of the indentation so as to make the measurement procedure inappropriate to obtain reasonable results. Ullner et all. [7] has shown that on the depth-sensing testing not seen this problem directly, but in case of chipping the indentation depth refers to a wrong load bearing area. For this reason, some preliminary instrumented tests were made at load of 2000 mN and the surfaces of both samples were subjected to an optical check to verify the absence of such damage.

Figs. 1 and 2 show the indents generated by the Vickers indenter at 2000 mN, onto ZTA and ATZ respectively. Micrographies show the absence of cracking or chipping in the surroundings of the residual indent.

Figs. 3 and 4 show typical load–depth curves at different indentation loads for ATZ and ZTA respectively. An overlapping of all the load–displacement curves can be observed for both ceramics, indicating a high level of reproducibility.

During unloading there is an elastic recovery of the area around the indent and then the final depth is reduced compared to one at the maximum indenter displacement. The difference between the maximum depth of indentation and the final depth of residual microhardness impressions, as a function of the indentation load, is shown in Fig. 5 for both materials. You can see how the depth of the indent increased by increasing indentation load. Moreover, by increasing materials microhardness, the indenter displacement at maximum load is reduced. This is the reason why ZTA shows a lower penetration than ATZ sample.

Fig. 6 shows the load/indentation depth as a function of indentation depth for both specimens. The curve reveals

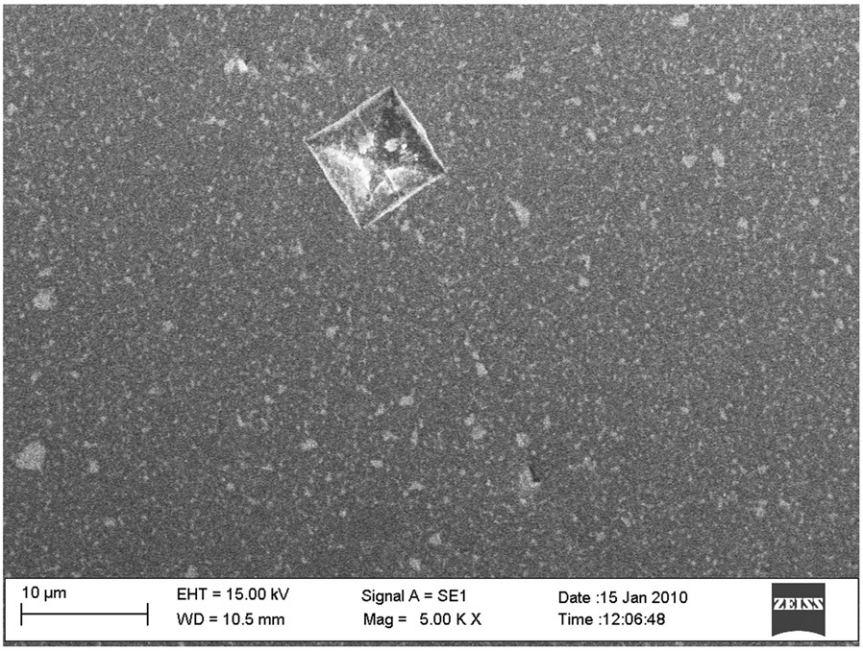

Fig. 1. SEM photograph of traditional Vickers impressions developed on surface of ZTA sample at 2000 mN.

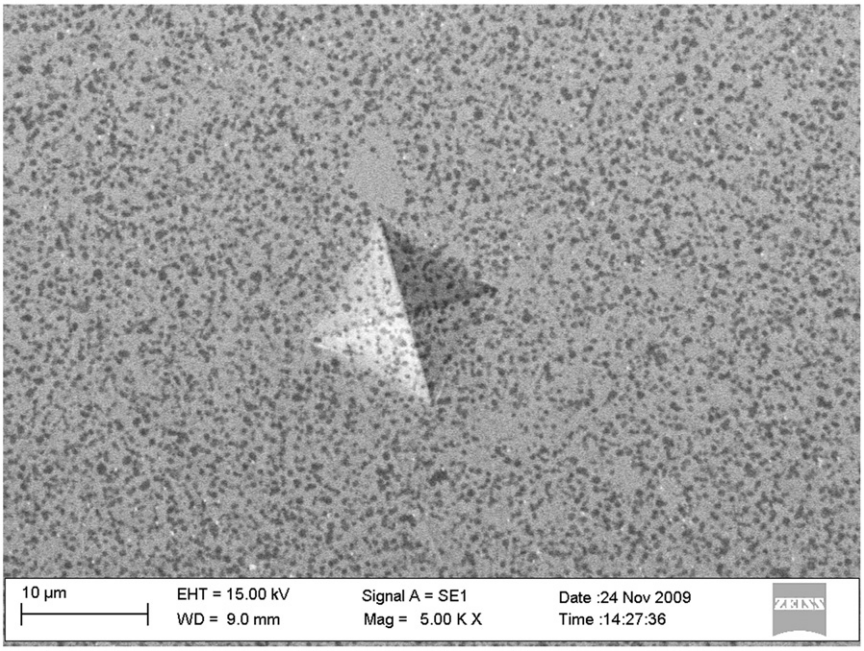

Fig. 2. SEM photograph of traditional Vickers impressions developed on surface of ATZ sample at 2000 mN.

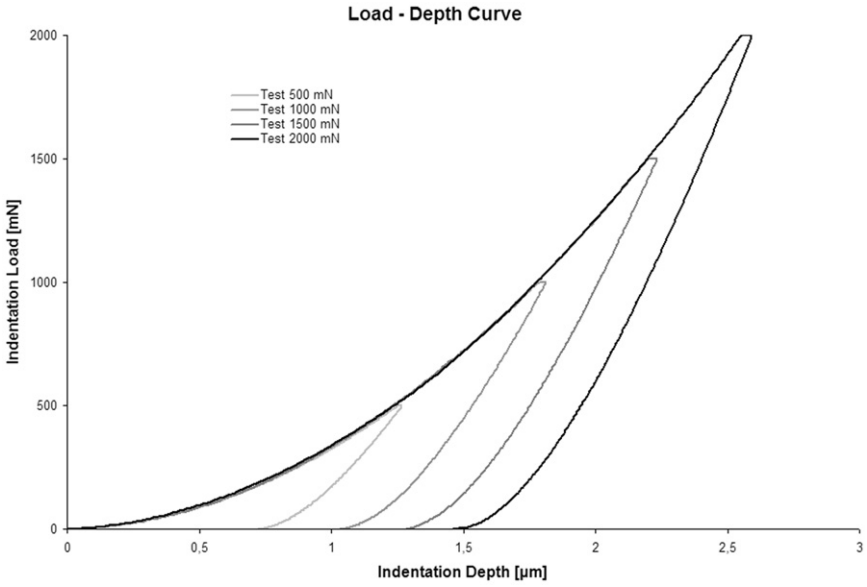

Fig. 3. Load-indentation depth curves of ATZ.

that there is linear correlation between F/D and D in the whole indentation range, indicating an indentation size effect. In the past, a good linear relationship between load indentation size and indentation size in the case of Vickers indentation [10] has been observed, and the results obtained in this study reflect this trend.

Unloading parts of the curves exhibit different slopes so that several Young's moduli were calculated (Tables 2 and 3) as for instrumented (HM, HV_{L-D}) and traditional (HV) microhardnesses. It can be noticed that differences among Young's Moduli are limited for both ceramics.

The influence of the indentation load on Young's modulus is reported in Fig. 7. The ZTA and ATZ showed values in the range of 348–339 and 266–260 GPa respectively. Comparing these values with those reported in the literature [17,18] there is a slight difference Young's modulus of ATZ and a big difference in that of the ZTA. You can see that the values of Young's modulus show an apparently insignificant dependence on the indentation load even if an apparent trend can be observed; increasing applied load Young's modulus tends to decrease in limited extent. Such a decrease is related to the slope

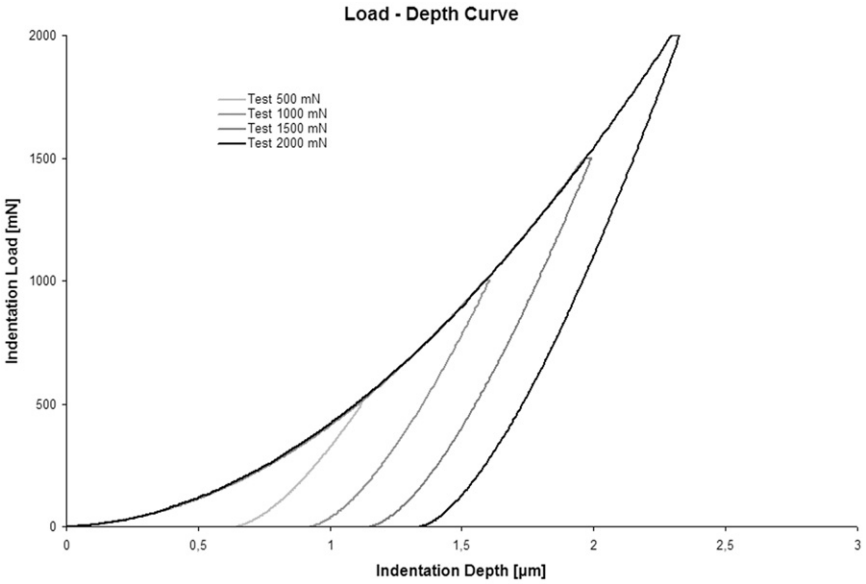

Fig. 4. Load-indentation depth curves of ZTA.

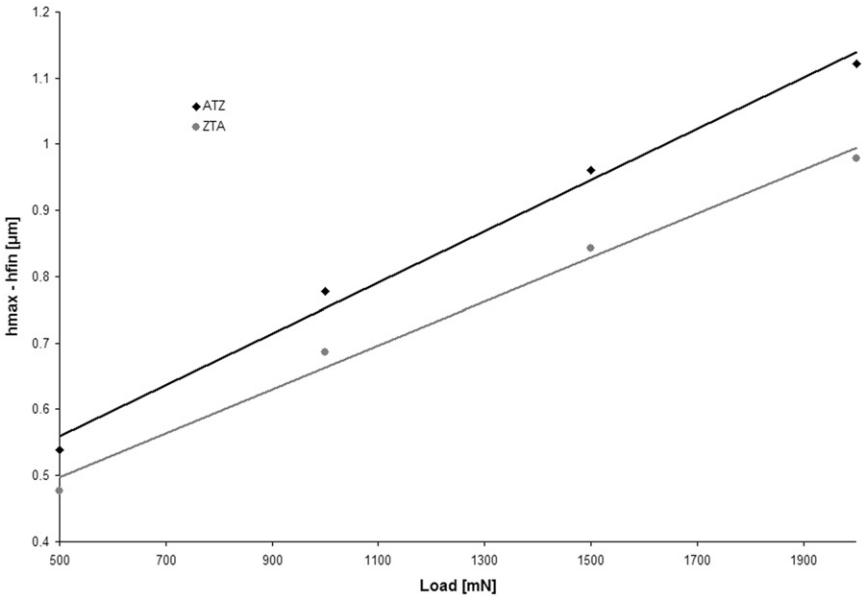

Fig. 5. Elastic recovery as a function of indentation load.

change of unloading segments of the curves. It has to be underlined here that, due to the difficulties in determining the slope with a high precision, the dependence on the indent load cannot be stated.

As for Martens microhardness, the low standard deviation observed indicate the reproducibility and accuracy of this method, proving that it eliminates subjective errors thanks to the possibility to measure the indentation depth under dynamic loading conditions.

The Figs. 8 and 9 show the influence of microindentation load on the microhardness of ZTA and ATZ materials respectively. Increasing indentation loads microhardness for both materials decreases, though not excessively.

According to Krell et al. [19] an indentation size effect can be observed. In fact, at lower indentation loads a higher resistance to plastic deformation can be observed, due to a reduction of the space available for the dislocation movement.

The indentation size effect has been examined extensively for microhardness testing of ceramic materials by several authors [10], which have provided some explanations for the such effect during microindentation, including surface sinking-in or pile-up [20,21], and indenter tip correction [22].

To explain the influence of microindentation load or depth on microhardness, we must consider the relationship

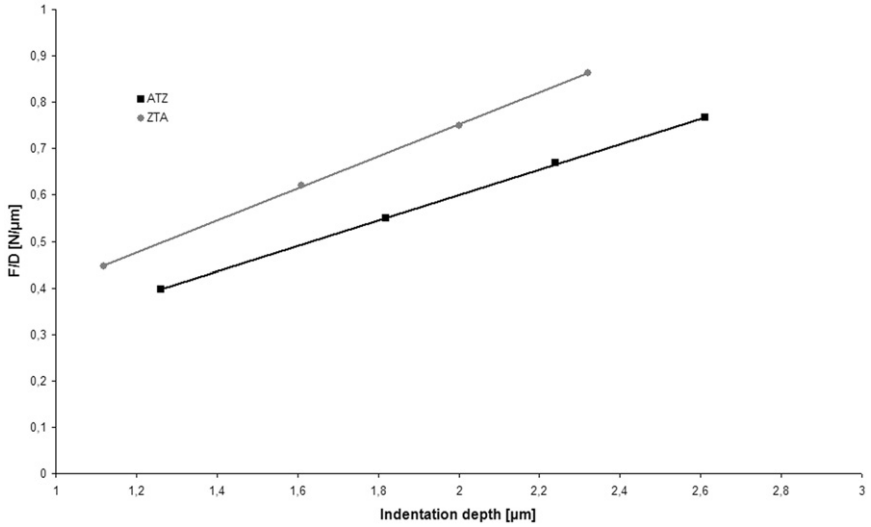

Fig. 6. Relationship between load over indentation depth and indentation depth in the loading segments of the load depth curves of ZTA and ATZ.

Table 2
Microhardness and Young's modulus for ZTA.

Load (mN)	500	1000	1500	2000	Average$_{(500-2000\ mN)}$
HM (GPa)	13.48	13.39	13.23	13.22	13.35 ± 0.13
HV_{L-D} (GPa)	21.97	21.81	21.51	21.44	21.71 ± 0.26
HV (Gpa)	22.80	22.14	22.01	21.91	22.35 ± 0.44
E_{IT} (Gpa)	348	344	340	339	344 ± 4.5

Table 3
Microhardness and Young's modulus for ATZ.

Load (mN)	500	1000	1500	2000	Average$_{(500-2000\ mN)}$
HM (GPa)	10.73	10.68	10.65	10.57	10.65 ± 0.08
HV_{L-D} (GPa)	17.10	17.04	16.99	16.81	16.95 ± 0.14
HV (GPa)	16.60	16.41	16.35	16.20	16.40 ± 0.20
E_{IT} (GPa)	266	263	262	260	263 ± 2.5

between load and indentation size, as it has been shown that there is proportionality between the indentation size and indentation depth at applied load. The load dependence can also be expressed through the application of power law:

$$F = A \times d^n$$

where F is the indentation load, d is the resulting indentation size, A and n are descriptive parameters derived from the curve fitting of experimental results [10]. This equation is sometimes referred to as Meyer's law [23] and it is known as the indentation size effect.

Analyzing the values of Vickers microhardness obtained by the traditional method, shown in Tables 2 and 3, and the influence of indentation load, reported in Figs. 8 and 9, you can see that in both cases we note the presence of the indentation size effect, although in the case of ATZ the variation of microhardness is linear and less pronounced.

Observing the difference between the traditional and instrumented methods at different indentation loads, a relationship between the conventional and instrumented Vickers microhardness can be observed. As generally to be expected for proper measurements, the resulting HV_{L-D} data for both ceramics come close to the HV values with only apparently insignificant deviations for both ATZ and ZTA. This deviation may be attributable to the optical perception of the operator during the measurement of the diagonals.

The instrumented Vickers microhardness was lower in comparison to the conventional Vickers microhardness for ZTA at all indentation loads. An opposite trend was observed in the case of ATZ. Indentation size effect in

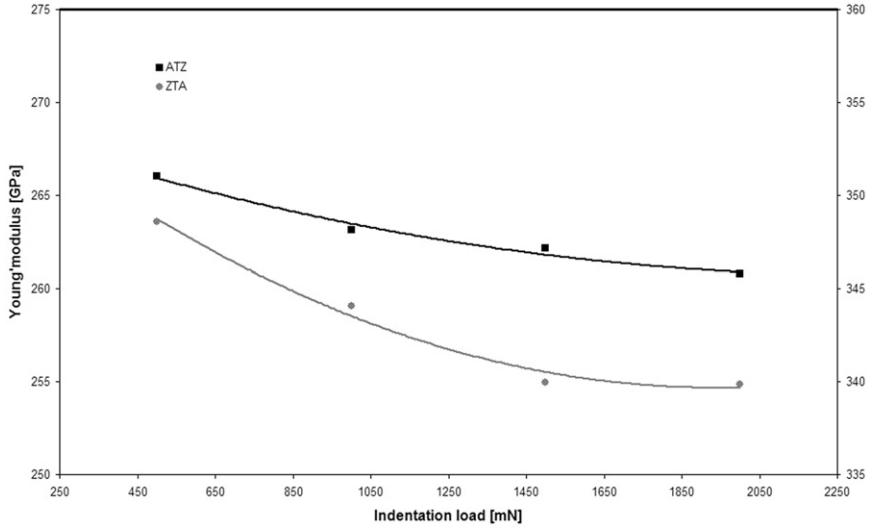

Fig. 7. Young's modulus as function of indentation load for ZTA and ATZ.

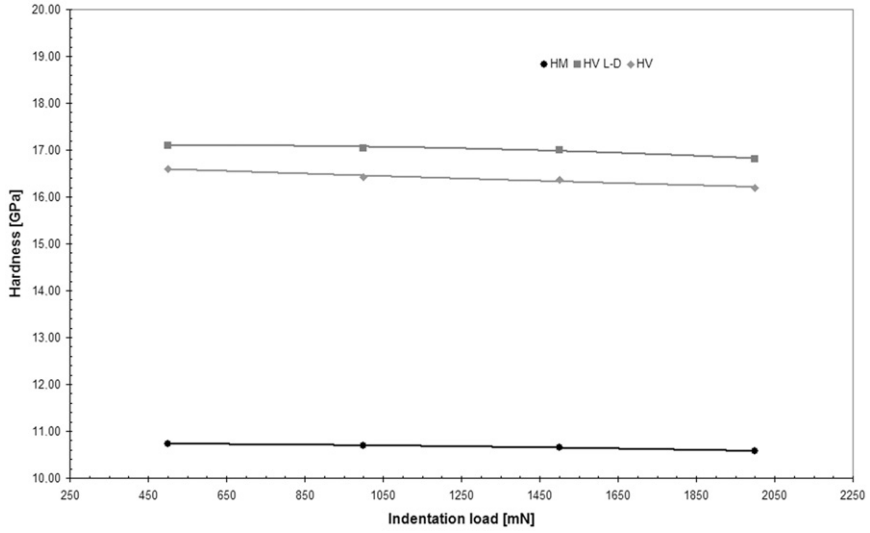

Fig. 8. Microhardness as a function of indentation load for ZTA.

sintered ATZ and ZTA is very small with an increase of the microhardness lower than 90 N/mm^2 between 500 and 2000 mN of load, as to be expected regarding the narrow range of maximum testing loads which differ by less than a factor of 10 in the present investigation.

4. Conclusion

A study of the load influence on Young's modulus and microhardness of sintered ZTA and ATZ ceramics has been conducted at low indentation loads by instrumented Vickers microindentation experiments and the Vickers traditional method. Young's modulus and microhardness were deduced by analyzing the unloading segments of the microindentation load–depth curves using the Oliver–Pharr method.

Both Young's modulus and microhardness showed an indentation load dependence. Load dependence of these mechanical properties of ceramic samples may be attributed to the indentation size effect. The results indicated that an indentation size effect also exists for microhardness obtained by traditional Vickers microindentation. The results of the present work confirm the previous experiences with zirconia [10] and alumina [11].

Since instrumented microhardness technique allows the evaluation of the elastic response after indenting by using the initial slope of the unloading curve, such method resulted more appropriate than traditional one to study the indentation response of ceramics. However, it does not

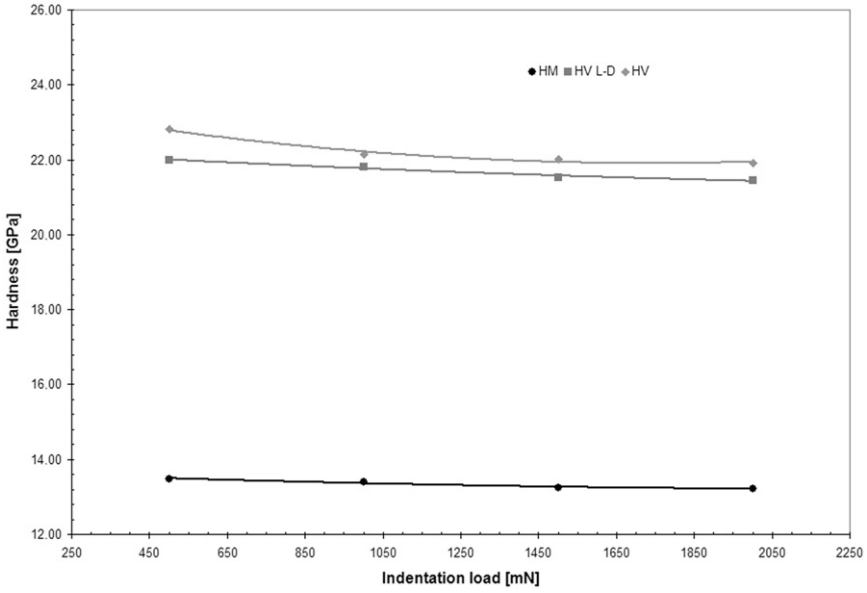

Fig. 9. Microhardness as a function of indentation load for ATZ.

currently provide a reduction of the error associated with optically derived measurements if there are chipping and cracking during the indentation test.

In summary, this fully automated test offers the advantages of simple and rapid recording compared to optical measurements of indent diagonal or diameter. Each indentation takes less than two minutes and the HM is calculated automatically using the instrument software.

Acknowledgments

The authors would like to thank Institute of Science and Technology for Ceramics for the preparation of the samples used in the tests and for the invaluable technical support.

References

[1] T. Linkevicius, E. Vladimirovas, S. Gybauskas, A. Puisys, V. Rutkunas, Venner fracture in implant-supported metal-ceramic restorations: part I: overall success rate and impact of occlusal guidance, Stomatologija—Baltic Dental and Maxillofacial Journal 10 (2008) 133–139.

[2] J.R. Kelly, I. Denry, Stabilized zirconia as a structural ceramic: an overview, Dental Materials 24 (2008) 289–298.

[3] J.R. Kelly, I. Denry, State of the art of zirconia for dental applications, Dental Materials 24 (2008) 299–307.

[4] J. Chevalier, What future for zirconia as a biomaterial?, Biomaterials 27 (2006) 535–543.

[5] A.H. De Aza, J. Chevalier, G. Fantozzi, Crack growth resistance of alumina, zirconia and zirconia toughened alumina ceramics for joint prostheses, Biomaterials 23 (2002) 937–945.

[6] R.M. Westrich, Use of the scanning electron microscope in microhardness testing of high-hardness materials, in: P.J. Blau, B.R. Lawn. (Eds.), Microindentation Techniques in Materials Science and Engineering, ASTM STP 889, American Society for Testing and Materials, Philadelphia, PA, 1986, pp. 196–205.

[7] C. Ullner, J. Beckmann, R. Morrell, Instrumented Indentation Test for Advanced Technical Ceramics, Journal of the European Ceramic Society 22 (2002) 1183–1189.

[8] A. Martens, Handbook of Materials Science for Mechanical Engineering, Springer, Berlin, 1898, p. 234.

[9] S.A. Shahdad, J.F. McCabe, S. Bull, S. Rusby, R.W. Wassell, Hardness measured with traditional vickers and martens hardness methods, Dental Materials 23 (2003) 1079–1085.

[10] B.K. Jang, Influence of low indentation load on Young's modulus and hardness of 4 mol% Y_2O_3–ZrO_2 by nanoindentation, Journal of Alloys and Compounds 426 (2006) 312–315.

[11] A. Krell, S. Schädlich, Nanoindentation hardness of submicrometer alumina ceramics, Materials Science and Engineering A 307 (2001) 172–181.

[12] W.C. Oliver, G.M. Pharr, An improved technique for determining hardness and elastic modulus using load and displacement sensing indentation experiments, Journal of Materials Research 7 (1992) 1564–1583.

[13] ISO 14577, Metallic materials—instrumented indentation test for hardness and materials parameters, International Organization for Standardization, Geneva, Switzerland, 2002.

[14] ASTM E 112—standard test methods for determining average grain size, 229–251.

[15] K.D. Bouzakis, N. Michailidis, Indenter Surface area and hardness determination by means of a FEM-supported simulation of nanoindentation, Thin Solid Films 494 (2006) 155–160.

[16] A. Krell, S. Schädlich, Depth sensing hardness in sapphire and in sintered sub-μm alumina, International Journal of Refractory Metals and Hard Materials 19 (2001) 237–243.

[17] M.G. Faga, A. Vallée, A. Bellosi, M. Mazzocchi, N.N. Thinh, G. Martra, S. Coluccia, Chemical treatment on alumina–zirconia composites inducing apatite formation with maintained mechanical properties, Journal of the European Ceramic Society 32 (2012) 2113–2120.

[18] W. Pabst, G. Ticha, E. Gregorova, E. Tynova, Effective elastic properties of alumina–zirconia composite ceramics, Silikaty 49 (2005) 77–85.

[19] A. Krell, A new look at the influences of load, grain size, and grain boundaries on the room temperature hardness of ceramics, International Journal of Refractory Metals and Hard Materials 16 (1998) 331–335.

[20] K. Zeng, E. Söderlund, A.E. Giannakopoulos, D.J. Rowcliffe, Controlled indentation: a general approach to determine mechanics properties of brittle materials, Acta Materialia 44 (1996) 1127–1141.
[21] A. Bolshakov, G.M. Pharr, Influences of pileup on the measurement of mechanical properties by load and depth sensing indentation, Journal of Materials Research 13 (1998) 1049.
[22] J. Thurn, R.F. Cook, Simplified area function for sharp indenter tips in depth-sensing indentation, Journal of Materials Research 17 (2002) 1143–1146.
[23] G.N. Babini, A. Bellosi, C. Galassi, Characterization of hot pressed silicon nitride based materials by microhardness measurements, Journal of Materials Research 22 (1987) 1687–1693.